

To what extent can dynamical models describe statistical features of turbulent flows?

V. Carbone¹, R. Cavazzana², V. Antoni^{2,3}, L. Sorriso-Valvo¹, E. Spada², G. Regnoli^{2,3}, P. Giuliani⁵, N. Vianello^{2,3}, F. Lepreti¹, R. Bruno⁶, E. Martines², P. Veltri¹

¹*Dipartimento di Fisica and Istituto di Fisica della Materia*

Università della Calabria, 87036 Rende (CS), Italy.

²*Consorzio RFX - Associazione Euratom-ENEA per la fusione, Padova, Italy.*

³*Istituto di Fisica della Materia, Unità di Padova, Italy.*

⁵*The Niels Bohr Institute and Danish Metereological Institute, DK-2100 Copenhagen, Denmark.*

⁶*Istituto di Fisica dello Spazio Interplanetario, Roma, Italy.*

(November 18, 2018)

Abstract

Statistical features of "bursty" behaviour in charged and neutral fluid turbulence, are compared to statistics of intermittent events in a GOY shell model, and avalanches in different models of Self Organized Criticality (SOC). It is found that inter-burst times show a power law distribution for turbulent samples and for the shell model, a property which is shared only in a particular case of the running sandpile model. The breakdown of self-similarity generated by isolated events observed in the turbulent samples, is well reproduced by the shell model, while it is absent in all SOC models considered. On this base, we conclude that SOC models are not adequate to mimic fluid turbulence, while the GOY shell model constitutes a better candidate to describe the gross features of turbulence.

PACS. 05.45.-a: Nonlinear dynamics and nonlinear dynamical systems

PACS. 05.65.+b: Self-organized systems

PACS. 52.35.Ra: Plasma turbulence

Turbulence in neutral and charged fluids exhibits bursty behaviour, power laws and $1/f$ spectra. Understanding the origin of the rich and complex dynamics underlying these properties, is a challenging and fascinating task. In the years different models have been proposed aimed to catch the fundamental mechanism of this phenomenology. Among them simplified models ("sandpiles") based on Self-Organized Criticality (SOC) [1] and dynamical systems approach [2], are particularly suitable for this purpose. SOC has been proposed as a paradigm for some complex systems, such as earthquakes, solar flares, river floods, fusion plasmas, etc. Despite the very simple governing rules, these systems exhibit a rich dynamics showing bursty behaviour with impulsive events ("avalanches" in sandpiles) which remind a variety of natural phenomena, including turbulence. Power laws are observed for the total energy [1,3,4], the duration and the peak energy distributions of the bursts [1] and for the total energy frequency spectra [5]. On the other hand models based on the dynamical systems approach have been developed by reducing the fluid equations, in order to isolate the basic mechanisms generating turbulence. An example of a model belonging to this class is the so called GOY shell model (see [2] and ref.s therein). This model describes a one dimensional fluid system by a set of ordinary differential equations of complex variables non linearly interacting through the coupling of the neighbour and next-neighbour modes.

To what extent these simplified models are good candidates to mimic turbulence is an intriguing question, reported, for example, in Ref.s [1,6-8]. The present paper is aimed to contribute to clarify this issue by comparing the predictions of these different dynamical models with samples of turbulence in neutral and charged fluids. The comparison is carried out by discussing two basic properties of turbulence, namely the presence of long time correlations and intermittency. For this purpose two statistical analysis tools have been used: the Distribution of the Waiting Times (WTD) Δt between subsequent bursts [6] and the comparison of the Probability Distribution Function (pdf) of fluctuations resolved at different time scales [9]. These methods have been applied to SOC and GOY models as well as to experimental data. In particular, concerning SOC models, we have analyzed successive generalization of the original sandpile model (BTW model), made by Kadanoff et al. [3]

which varied the underlying microscopic rules and by Hwa and Kardar [10] which included finite drive effects (the running sandpile).

It is worth noticing that the analysis of dynamical properties of these models requires a correct definition of the timescale, a point often neglected in SOC literature. For example Ref. [3] does not give any definition of the timescale, since it is focused on integral properties of avalanches, namely the total released energy and particles. With this in mind we choose to introduce in Kadanoff sandpile the same timescale definition proposed in Ref. [4]. Accordingly in this case we built the signal of dissipated energy $\epsilon_K(t)$ considering every avalanche as an instantaneous event, with an amplitude equal to the integral avalanche size and the time between two subsequent events proportional to the number of particles needed to put the system in the unstable state again. On the other hand in the case of the running sanpile [10] the dissipated energy signal and its timescale are clearly defined. In each temporal step the system is continuously fed at random with a certain finite deposition rate probability J_{in} and the unstable sites are simultaneously updated. The dissipated energy signal $\epsilon_H(t)$ in this case is taken as the total number of unstable sites at each step. The timescale of the previous model is recovered in the limit $J_{in} \rightarrow 0$. In our simulation we consider a sandpile of size ℓ , and associate to each lattice site n the height of the pile $h(n, t)$. If there is any unstable site according to the rule $h(n, t) - h(n \pm 1, t) > \Delta$, the system is evolved by taking a fixed amount N_f of sand from the unstable n site and redistributing grains to the neighbouring $n \pm 1$ site (we set the threshold $\Delta = 50$ and $N_f = 20$).

The WTD $P(\Delta t)$ for the Kadanoff model (right-hand panel of Fig. 1) shows a clear exponential decay. This behaviour, which is known to be associated to independent Poissonian events [6], indicates that no long term correlations are present between subsequent avalanches, as found in the standard BTW model [6].

In the case of running sanpile at small J_{in} , an exponential WTD was found (top right-hand panel of Fig. 2), recovering the behaviour of the Kadanoff sanpile. On the other hand, increasing the drive J_{in} a tendency to a power law behaviour $P(\Delta t) \sim \Delta t^{-1.5}$ emerges. In order to measure the waiting times, we note that while at $J_{in} \rightarrow 0$ avalanches are isolated

events so that waiting times coincide with quiescent intervals, at high J_{in} there is a continuous activity. Thus to define the waiting times between subsequent events a threshold has been chosen applying the algorithm reported in [6]. The waiting time corresponds to the time interval between two subsequent events with amplitude beyond this threshold. In the limit $J_{in} \rightarrow 0$ this method correctly gives threshold 0.

It is known that long range time correlations can be obtained by overlapping signals from uncorrelated avalanches [17,11]. In order to test the origin of the power law above reported, following a procedure originally proposed in ref. [1], a signal has been generated by randomly overlapping isolated avalanches for the case $J_{in} \rightarrow 0$, keeping an average dissipation rate equal to that for the case $J_{in} = 4$. In this case an exponential decay of the WTD has been found. Thus we conclude that the origin of power law in the WTD of the Hwa-Kardar model is due to the interaction among the avalanches inside the system. The emerging of a power law behavior with exponent close to $\beta \simeq 1.5$ in the WTD is a common feature found for all Hwa-Kardar systems, independently from their size ℓ .

In order to characterize the properties of the dynamics of these SOC systems, the energy fluctuations $\delta\epsilon_\tau = \epsilon(t + \tau) - \epsilon(t)$ at different scales τ of the energy signal $\epsilon(t)$ defined above have been analysed. The increments $\delta\epsilon_\tau$ of a stochastic process are self-similar with respect to the scaling transformation $\tau \rightarrow \lambda\tau$ (with $\lambda > 0$) if $\delta\epsilon_\tau \sim \lambda^{-\alpha}\delta\epsilon_{\lambda\tau}$ [9], which means that the cumulative distributions of the first and the second term coincide for a given scaling exponent α . This can be translated on the relationship between density probability of increments at two different scales τ , namely $pdf(\delta\epsilon_\tau) = \lambda^{-\alpha}pdf(\lambda^{-\alpha}\delta\epsilon_{\lambda\tau})$. Test for self-similarity of random processes can be made without actually assuming a value for α . In fact it can be shown that pdfs of rescaled fluctuations $\delta E_\tau = \delta\epsilon_\tau/\sigma_\epsilon(\tau)$, where $\sigma_\epsilon(\tau) = \{\langle[\epsilon(t+\tau) - \epsilon(t)]^2\rangle\}^{1/2}$ (brackets being time averages), are invariant in a self-similar process, say $pdf(\delta E_\tau) = pdf(\delta E_{\lambda\tau})$ [9].

The pdfs of the fluctuations δE_τ at different scales τ for the Kadanoff sandpile are shown on the left-hand panel of Fig. 1. The bursty appearance of SOC signals is reflected onto the shape with fat tails of the pdfs. However pdfs are invariant when plotted in the rescaled form, so the process turns out to be purely self-similar.

Concerning the running sandpile, in the case of small drive ($J_{in} \rightarrow 0$) the result turns out to be close (upper-left panel of Fig. 2) to the Kadanoff model, confirming that in the above limit the two models are equivalent.

In the case of finite drive (bottom-left panel of Fig. 2), the shape of pdfs approaches a Gaussian shape due to the interaction of the avalanches, and, even more noticeable, the underlying process remains purely self-similar. These results are consistent with the intrinsic self-similar structure of SOC models [1], which is at the origin of its power law distributions and scaling properties [3]. It is worth noticing that self similarity is observed even in the case of finite drive, despite the common belief that "the true SOC behaviour arises only in the limit that the forcing rate approaches 0" [17,11].

The MHD GOY shell model [12] describes the dynamic of the energy cascade in turbulence. The wavevector space is divided in N shells, each shell being characterised by a discrete wavevector $k_n = 2^n k_0$ ($n = 0, 1, \dots, N$), and by the (complex) dynamical variables, velocity $u_n(t)$ and magnetic field $b_n(t)$, which represent characteristic fluctuations across eddies at the scale $\ell_n \sim k_n^{-1}$. The dynamical behaviour of the model is described by the following set of ordinary differential equations

$$\begin{aligned} \frac{du_n}{dt} = & -\nu k_n^2 u_n + ik_n \left\{ (u_{n+1} u_{n+2} - b_{n+1} b_{n+2}) \right. \\ & \left. - \frac{1}{4} (u_{n-1} u_{n+1} - b_{n-1} b_{n+1}) - \frac{1}{8} (u_{n-2} u_{n-1} - b_{n-2} b_{n-1}) \right\}^* + f_n \end{aligned} \quad (1)$$

$$\begin{aligned} \frac{db_n}{dt} = & -\eta k_n^2 b_n + \frac{ik_n}{6} \left\{ (u_{n+1} b_{n+2} - b_{n+1} u_{n+2}) \right. \\ & \left. + (u_{n-1} b_{n+1} - b_{n-1} u_{n+1}) + (u_{n-2} b_{n-1} - b_{n-2} u_{n-1}) \right\}^* \end{aligned} \quad (2)$$

ν and η are the kinematic viscosity and the resistivity respectively, and f_n is an external forcing term. The nonlinear terms have been obtained by imposing quadratic nonlinear coupling between neighbouring shells and the conservation of three ideal invariants. Detailed informations on the model and on simulations can be found in Ref.s [6,12].

The model has a fixed point in the form of a Kolmogorov-like scaling $u_n \sim b_n \sim k_n^{-1/3}$, and exhibits a chaotic dynamics on a strange attractor in the phase space around the fixed

point. This is due to the presence of the ideal invariants. What is interesting here is the fact that fluctuations of the degree of chaoticity in the model generate a multifractal probability measure on the attractor. As a consequence the statistics of a sample of turbulence coming from simulations of the system is characterised by multifractal scalings, and this manifest itself as a breakdown of self-similarity of the system. That is, at variance with sandpile models, pdfs of the rescaled variables $\delta u_n = \text{Real}\{u_n\}/\sigma_{u_n}(\ell_n)$ and $\delta b_n = \text{Real}\{b_n\}/\sigma_{b_n}(\ell_n)$ (see figure 3) strongly depend on the scale ℓ_n . At large scales pdfs are gaussian, while they tend to develop fat tails for small ℓ_n , towards the dissipative range. The departure from gaussianity visible at smaller scales, is due to bursts localised in time, which can be identified and extracted through an iterative procedure on $|u_n|^2$ and $|b_n|^2$, described extensively in Ref. [6]. The WTD for these events is shown in the bottom panels of figure 3. We found a power law $P(\Delta t) \sim \Delta t^{-\beta}$ over at least two decades (the scaling exponents β are reported on the figures). Long-range correlations between bursts are the origin of the power law for waiting times.

We proceed now to investigate some samples of turbulent flows. First of all we consider a sample of turbulence as measured in the atmospheric boundary layer [13], where the longitudinal velocity field $u(t)$ is recorded. Then we consider two samples of magnetic field intensity $B(t)$ in plasmas as recorded both in a given low-speed stream of the solar wind by Helios II spacecraft [14], and in a laboratory device for thermonuclear fusion research (the RFX experiment [15]). Even if turbulent samples are collected in very different physical conditions, they show the same statistical properties. The rescaled fluctuations, namely $\delta u_\tau = [u(t + \tau) - u(t)]/\sigma_u(\tau)$ and $\delta B_\tau = [B(t + \tau) - B(t)]/\sigma_B(\tau)$, depend on the scale τ (figure 4). At large scales pdfs are gaussian, while they tend to develop fat tails as $\tau \rightarrow 0$, towards the dissipative range. The departure from gaussianity, which results in a correction to the usual Kolmogorov scaling laws, is due to "intermittency in fully developed turbulence" (see Ref. [9,16] and references therein). Since at smaller scales the wings of pdfs increase, intermittency is represented by intense and localised fluctuations which accumulates at smaller scales. These "events" are generated during the turbulent energy cascade,

and can be interpreted as due to a non homogeneous breakdown of "eddies" towards small scales [16]. Their presence originates the departure from a pure self-similarity of fluctuations at the various scales. The time of occurrence of the events in a turbulent flow can be extracted through the procedure described in Ref. [6], and the distribution of waiting times between them is shown in the bottom panels of figure 4 for the different samples. A power law over two decades, with non universal scaling exponents β , is found in all samples.

To summarize, we found that turbulence and the GOY MHD shell model always show power law for WTD, while this property is shared only by a SOC model, namely the running sandpile in the "strong" feeding regime, far from BTW limit [1,11]. Moreover pdfs of rescaled fluctuations in both BTW and other SOC models do not change shape with the scale τ . On the contrary intermittency in turbulent flows manifests itself as a breakdown of a pure self-similarity, leading to increasingly non gaussian tails for pdfs as the scale becomes smaller. The same phenomenon is observed in the GOY shell model, and is due to "time intermittency". Non linear terms in the model, which conserve some few invariants, are responsible for the occurrence of bursts of chaoticity which are concentrated on the dissipative shells [18]. Such typical behaviour in the shell model generates a breaking of the global scaling invariance of the model, and this results in a correction to the Kolmogorov-like scaling law. This correction has the same statistical effects of the corrections of the Kolmogorov scaling laws due to usual intermittency in real fluid flows. Then as far as the statistical properties we investigated are concerned, SOC models we examined do not adequately mimic neither fluid nor plasma turbulence. On the contrary time intermittency in the GOY shell model allows the model to capture the gross statistical features of real turbulence.

REFERENCES

- [1] P. Bak, C. Tang, and K. Wiesenfeld, Phys. Rev. Lett. **59**, 381 (1987).
- [2] T. Bohr, M.H. Jensen, G. Paladin, and A. Vulpiani, *Dynamical Systems Approach to Turbulence* (Cambridge University Press, Cambridge, UK, 1998).
- [3] L.P. Kadanoff, S.R. Nagel, L. Wu and S.M. Zhou, Phys. Rev. A **39**, 6524 (1989).
- [4] Z. Olami, H.J. Feder and K. Christensen, Phys. Rev. Lett. **68**, 1244 (1992); K. Christensen and Z. Olami, J. Geophys. Res. B **97**, 8729 (1992).
- [5] H.J. Jensen, K. Christensen, H.C. Fogedby, Phys. Rev. B **40**, 7425 (1989).
- [6] G. Boffetta *et al.*, Phys. Rev. Lett. **83**, 4662 (1999).
- [7] M.P. Freeman, N.W. Watkins, and D.J. Riley, Phys. Rev. E **62**, 8794 (2000).
- [8] V. Antoni *et al.*, Phys. Rev. Lett. **87**, 045001 (2001).
- [9] C.W. Van Atta and J. Park, Lecture Notes in Physics **12**, 402 (1975).
- [10] T. Hwa and M. Kardar, Phys. Rev. A **45**, 7002 (1992).
- [11] H.J. Jensen, *Self-Organized Criticality*, Cambridge University Press, Cambridge (1998).
- [12] P. Giuliani, and V. Carbone, Europhys. Lett. **43**, 527 (1998); P. Giuliani, *Shell models of MHD turbulence cascade*, PhD Thesis, Università della Calabria (1999).
- [13] Albertson *et al.*, Phys. Fluids **10**, 1725 (1998).
- [14] L. Sorriso-Valvo *et al.*, Geophys. Res. Lett. **23**, 121 (1996).
- [15] V. Carbone *et al.*, Phys. Rev. E **62**, R49 (2000).
- [16] U. Frisch, *Turbulence: the legacy of A.N. Kolmogorov*, Cambridge University Press, Cambridge (1995).
- [17] J. A. Krommes, Phys. Plasmas **7**, 1752 (2000).

[18] M.H. Jensen, G. Paladin, and A. Vulpiani, Phys. Rev. A **43**, 798 (1991).

FIGURES

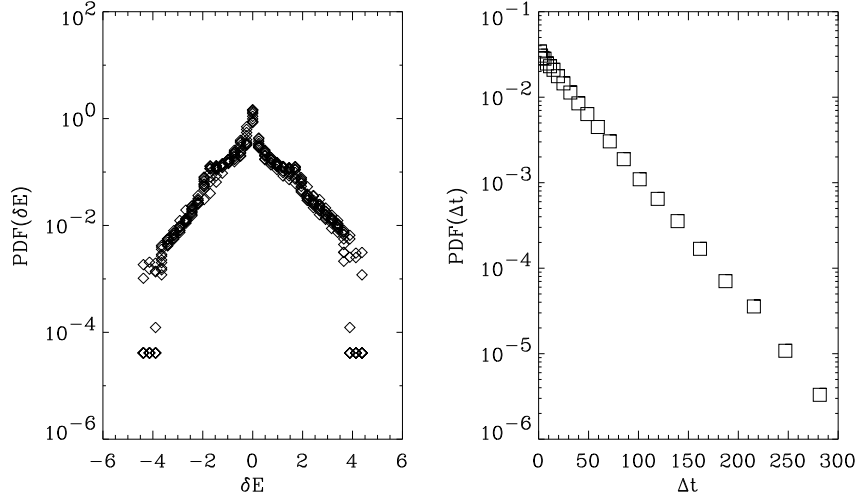


FIG. 1. We show the results obtained from the Kadanoff “local limited” sandpile obtained with a system size $\ell = 1024$. In the left panel we show the pdfs of the rescaled fluctuations at different scales τ , and in the right panel (log–lin plot) we show the distribution of waiting times between avalanches. Simulations obtained with different values of ℓ show the same results.

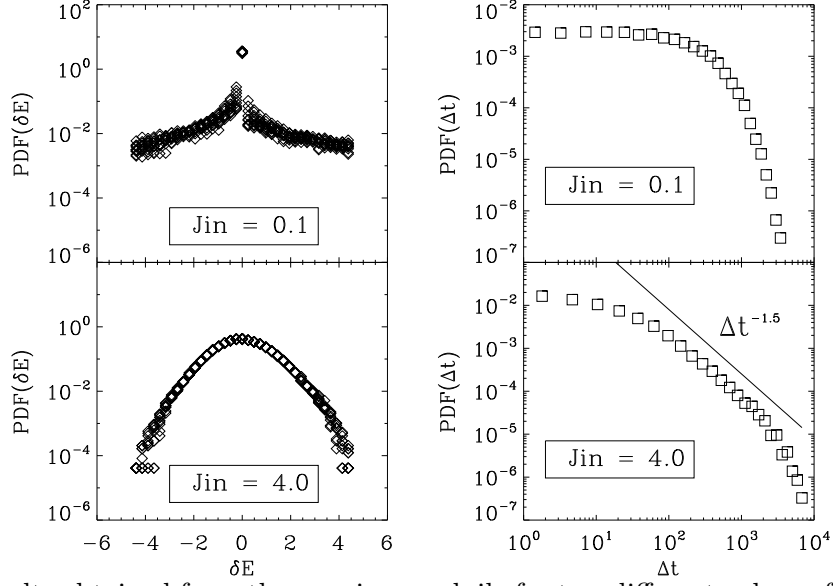


FIG. 2. Results obtained from the running sandpile for two different values of J_{in} (see text). In the left panels we show the pdfs of the rescaled fluctuations at different scales τ , and in the right panels (log-log plot) we show the distribution of waiting times between avalanches.

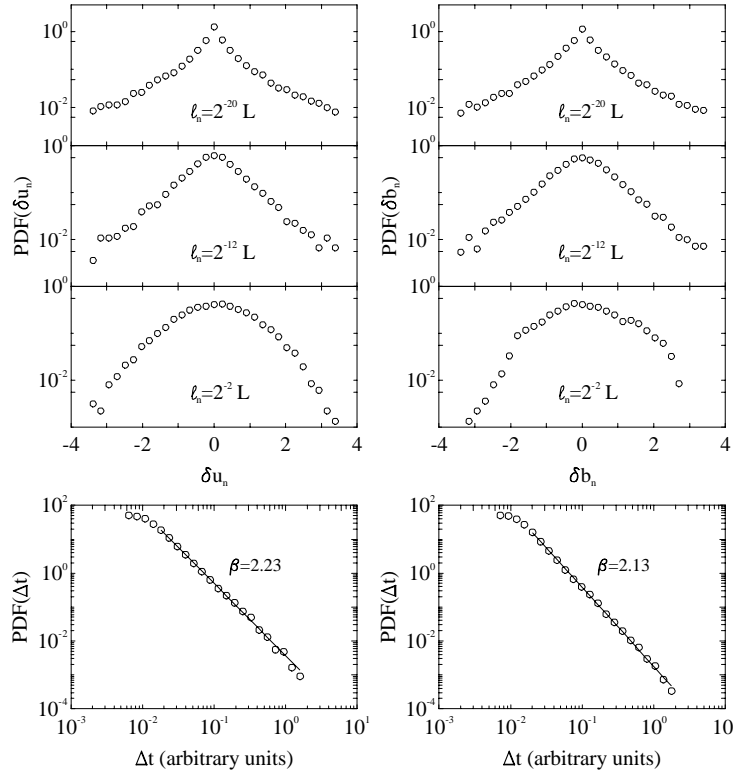


FIG. 3. We show results obtained from simulations of the GOY MHD shell model. Left-hand and right-hand columns refer to velocity and magnetic variables respectively. In the first three panels of each column we show the pdfs of the rescaled dynamical variables at three different scales. In the bottom panels of each column we report the distribution of waiting times between events at the scale $\ell_n/L = 2^{-20}$ (where $L = k_0^{-1}$). The values of β represent the best fits of the power laws.

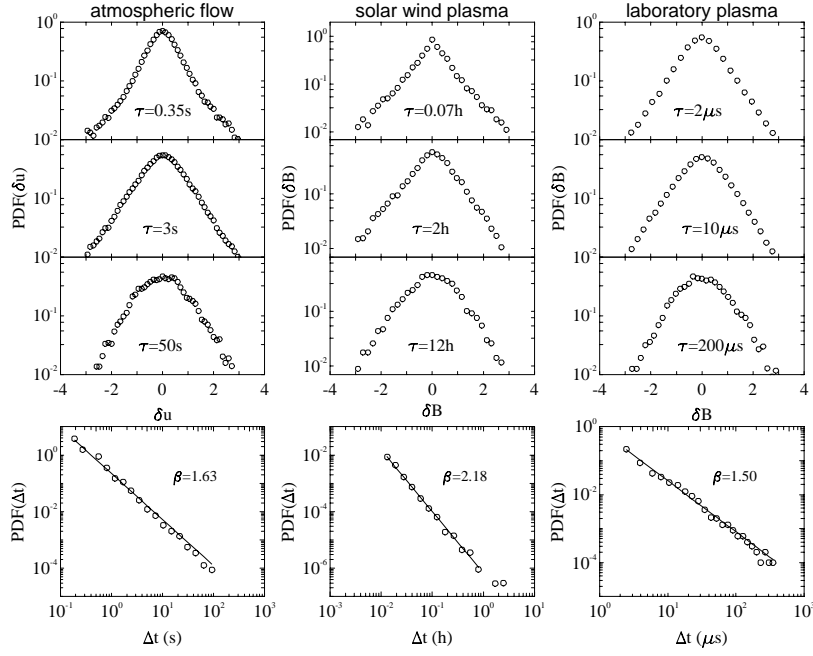


FIG. 4. Results obtained from a sample of fluid turbulence (left-hand column), a sample of magnetic turbulence measured by the Helios II satellite in the interplanetary space at distance $R = 0.9$ Astronomical Units (central column), and a sample of magnetic turbulence measured in a magnetically confined plasma in Reversed Field Pinch configuration (right-hand column). In the first three panels of each column we show the pdfs of the rescaled dynamical variables at three different scales. In the bottom panels of each column we report the distribution of waiting times between events at the smallest scale. The values of β represent the best fits of the power laws.